

Weakly relativistic dielectric tensor for arbitrary wavenumbers

Francesco Volpe*

Max-Planck-Institut für Plasmaphysik, D-17491 Greifswald, Germany

(Dated: October 16, 2007)

Abstract

The validity of Shkarofsky's dielectric tensor is extended by taking the strictly weakly relativistic limit and removing, when possible, assumptions on the wavenumbers along and across the ambient magnetic field, k_{\parallel} and k_{\perp} . An approximation of the time integral is retained, but is shown to be valid under more benign assumptions than those of quasi-perpendicular incidence and small Larmor radius. The increased generality with respect to k_{\parallel} permits to handle cases of comparable Doppler and relativistic widths of electron cyclotron resonances. The tensor also suits Bernstein waves, as it captures both their natural large k_{\perp} and the finite k_{\parallel} that is typical of some mode conversions, or acquired as a consequence of the large k_{\perp} when propagating in curved magnetic fields. Finally, relativistic corrections to the optimal angle for the ordinary-extraordinary-Bernstein mode conversion are presented.

I. INTRODUCTION

The relativistic dielectric tensor ϵ was first obtained by Trubnikov by solving the relativistic Vlasov equation in terms of a small perturbation to a Maxwellian distribution¹. A more treatable weakly relativistic approximation was then derived by Dnestrovskii for propagation perpendicular to the magnetic field². Later, this was extended by Shkarofsky to quasi-perpendicular incidence, such that³

$$N_{\parallel} \ll \beta_T \ll 1, \quad (1)$$

$$|N_{\parallel}(2\delta - N_{\parallel}^2)| \ll \beta_T^2. \quad (2)$$

Here N_{\parallel} is the parallel refractive index, $\beta_T^2 = k_B T / mc^2$ the squared thermal velocity in c units and $\delta = (\omega - n\omega_c) / \omega$ indicates the distance from the n -th cyclotron harmonic in dimensionless units.

In addition to making these hypotheses on N_{\parallel} , Shkarofsky's and most subsequent weakly relativistic formulations also expand ϵ as a power series in the (small) Larmor radius parameter³⁻¹¹

$$\lambda = \left(\frac{N_{\perp} \beta_T}{Y} \right)^2 < 1 \quad (3)$$

or take the opposite, asymptotic limit $\lambda > 1^{12,13}$. Here $Y = \omega_c / \omega$ is the dimensionless magnetic field. These series are formally correct, in the sense that, if they converge, they do so to an exact result. Convergence is ensured in one case by $\lambda < 1$ and in the other by $\lambda > 1$, so that, for any λ , one can always choose a converging expansion of ϵ in cyclotron harmonics. In practice, however, these series will be truncated and provide approximate results, valid in the $\lambda \ll 1$ or $\lambda \gg 1$ limit, respectively. The fewer the terms retained in the sum, the smaller is the range of validity in λ . Of course expressions, available in literature, which are already truncated, have a reduced range of validity. All these series expansions and truncated sums are summarized in Table I, and some of them were reviewed in¹⁴. In Table I we also note that not the whole ϵ but only an electrostatic approximation is considered in¹¹⁻¹³. Apart from a very general but numerically expensive series in a 4D space multiplied by a sum in a 2D space and a double combinatoric sum¹⁵, some approximations may not be adequate for electron Bernstein waves, as these waves are characterised by $\lambda \gtrsim 1$ and are excited/detected at finite N_{\parallel} ¹⁶⁻¹⁹ or tend to develop finite N_{\parallel} anyway, including values

$N_{\parallel} \geq 1$ ^{19,20}. Finite values of N_{\parallel} , of the order of β_T , are also encountered in ion Bernstein waves, for which they were treated numerically with the aid of root finders²¹.

Electromagnetic electron cyclotron waves propagating at intermediate angles relative to the magnetic field may also have $N_{\parallel} \approx \beta_T$. In this case the two mechanisms resolving the electron cyclotron emission/absorption line coexist and the fully relativistic ϵ , which embodies both the Doppler broadening and relativistic mass gain, should be invoked. However, because it is very complicated and not in a closed form, an analytic semi-relativistic form of ϵ valid for arbitrary values of N_{\parallel} and N_{\perp} is derived in the present work. Note that simplified 1D relativistic descriptions are available, for example for reflectometry²². However, modelling in 3D requires either the fully¹ or weakly^{3-8,8-13,15} relativistic dielectric tensor. Here a compromise is proposed between the generality of the full tensor and the ease of calculation of the weakly relativistic one.

Two well-known weakly relativistic approximations³⁶ are compared in Sec.II and the most rigorous is adopted. Only the strict weakly relativistic limit $\beta_T \ll 1$ is taken here. Unlike other works, the treatment is not restricted to $N_{\parallel} \ll \beta_T$, that would help isolating relativistic effects from Doppler ones, but is not the most general assumption. A cyclotron harmonic expansion is operated in Sec.III. The arbitrariness of N_{\parallel} leads to a further generalization of the generalized Shkarofsky functions and to new, N_{\parallel} -dependent terms in ϵ . In Sec.IV, this new mildly relativistic expression is compared with earlier results. Both warm and Shkarofsky formulas, in particular, are reobtained as limiting cases. This implies the new tensor to be valid for both oblique, Doppler-dominated injection and perpendicular, relativistically broadened absorption.

Sec.IV also shows that the generalization introduced in Sec.III is equivalent to perturb the arguments of the Bessel functions, which cannot be factored out of the integral anymore. Numerical results in Sec.V illustrate the broader domain of applicability of the new expression with respect to N_{\parallel} and N_{\perp} , at a modest computational extra cost. Finally, some calculations pertinent to Sec.III are reported in Appendix.

II. WEAKLY RELATIVISTIC LIMIT

The steady-state solution of the linearized Vlasov-Maxwell problem for a uniformly magnetized plasma is^{1,8}:

$$\epsilon_{ij} = \delta_{ij} + \frac{iX}{\beta_T^2} \int_0^\infty d\tau I_{ij}(\tau) \quad (4)$$

where $X = \omega_p^2/\omega^2$ is the non-dimensional density and τ the time renormalized to the wave period ω^{-1} . Apart from a factor nY , τ coincides with the gyrophase and, for practical uses, it is sufficient to integrate Eq.4 over a time τ long enough for the wave-particle interaction to take place, bearing in mind that correlation is destroyed after a certain number of gyroperiods.

The function $I_{ij}(\tau)$ is defined as an integral over the normalized momentum $\mathbf{u} = \mathbf{p}/mc$:

$$I_{ij} = T_{jk}^{(1)} \int \frac{d^3\mathbf{u}}{\gamma} u_i u_k f(\mathbf{u}) \exp(i\gamma\tau - i\mathcal{N} \cdot \mathbf{u}) \quad (5)$$

where $\gamma = \sqrt{1 + \mathbf{u}^2}$ is the Lorentz factor and the convention of implicitly summing on repeated indices is adopted. The tensor

$$T^{(1)} = \begin{pmatrix} \cos Y\tau & -\sin Y\tau & 0 \\ \sin Y\tau & \cos Y\tau & 0 \\ 0 & 0 & 1 \end{pmatrix} \quad (6)$$

defines a rotation of the reference frame at an angular frequency equal to the (normalized) gyrofrequency $Y = \omega_c/\omega$ around the field-aligned axis z . The remaining axes are chosen to yield $\mathbf{N} = (N_\perp, 0, N_\parallel)$. Finally,

$$\mathcal{N}_x = \frac{N_\perp}{Y} \sin Y\tau \quad (7)$$

$$\mathcal{N}_y = \frac{N_\perp}{Y} (\cos Y\tau - 1) \quad (8)$$

$$\mathcal{N}_z = N_\parallel \tau \quad (9)$$

and, for a thermal relativistic plasma, the distribution function equals

$$f(\mathbf{u}) = \frac{\exp(-\gamma\beta_T^{-2})}{4\pi\beta_T^2 K_2(\beta_T^{-2})} \quad (10)$$

where K_2 is the modified Bessel function of the second kind of order 2, also known as MacDonald function²³.

All parameters and independent variables in integral Eq.5 are real, apart from the refractive index components which are complex, with $\Re(N_\perp) \geq 0$.

Integration over momenta gives¹:

$$I_{ij} = \frac{\beta_T^{-2}}{K_2(\beta_T^{-2})} \left[T_{ij}^{(1)} \frac{K_2(R^{1/2})}{R} - T_{ij}^{(2)} \frac{K_3(R^{1/2})}{R^{3/2}} \right] \quad (11)$$

where

$$R = b^2 + \mathcal{N}^2 = \frac{1}{\beta_T^4} - \frac{2i}{\beta_T^2} \tau + 2 \frac{N_\perp^2}{Y^2} (1 - \cos Y\tau) + (N_\parallel^2 - 1)\tau^2, \quad (12)$$

$$b = \frac{1}{\beta_T^2} - i\tau \quad (13)$$

and $T_{ij}^{(2)} = (-)^{j+1} \mathcal{N}_i \mathcal{N}_j = \mathcal{N}_i T_{jk}^{(1)} \mathcal{N}_k$ is the tensor

$$T^{(2)} = \begin{pmatrix} \mathcal{N}_x^2 & \mathcal{N}_x \mathcal{N}_y & \mathcal{N}_x \mathcal{N}_z \\ -\mathcal{N}_x \mathcal{N}_y & -\mathcal{N}_y^2 & -\mathcal{N}_y \mathcal{N}_z \\ \mathcal{N}_x \mathcal{N}_z & \mathcal{N}_y \mathcal{N}_z & \mathcal{N}_z^2 \end{pmatrix}. \quad (14)$$

A. Weakly relativistic limit of Eq.11

Eq.4 with I_{ij} as in Eq.11, is known as the second of Turbnikov's formulas. The essential step in its weakly relativistic approximations^{3,7,13} is to assume the argument R of the modified Bessel functions to be large.

Clearly, from Eq.12, R is a function of the independent variables β_T , N_\parallel and N_\perp and at this stage the $\beta_T \rightarrow 0$ limit can be taken without implications for the other (orthogonal) directions N_\parallel and N_\perp . In particular, it is not necessary to assume small Larmor radii (Eq.3) and/or quasi-perpendicular incidence (Eq.1). The strict mildly relativistic limit $\beta_T \ll 1$ is sufficient, although not necessary, for $R \gg 1$. In turn, this justifies the asymptotic expansion²³

$$K_\nu(R^{1/2}) \simeq \sqrt{\frac{\pi}{2}} \frac{e^{-R^{1/2}}}{R^{1/4}} \left\{ 1 + \sum_{n=1}^{\infty} \frac{\prod_{p=1}^n [4\nu^2 - (2p-1)^2]}{n!(8R^{1/2})^n} \right\} \quad (15)$$

where, for the case of interest, $\nu = 2$ or 3 .

With this, Eq.11 becomes:

$$I_{ij} = \frac{e^{\beta_T^{-2}}}{\beta_T^3 + \frac{15}{8}\beta_T^5 + \frac{105}{128}\beta_T^7} e^{-R^{1/2}} Q_{ij} \quad (16)$$

$$Q_{ij} = \frac{T_{ij}^{(1)}}{R^{5/4}} \left(1 + \frac{15}{8R^{1/2}} + \frac{105}{128R} \right) - \frac{T_{ij}^{(2)}}{R^{7/4}} \left(1 + \frac{35}{8R^{1/2}} + \frac{945}{128R} \right) \quad (17)$$

The square root at exponent here, $e^{-R^{1/2}}$, poses a major difficulty for the integration of Eq.4. Factorizing $e^{-R^{1/2}} \simeq e^{-b}e^{-\mathcal{N}^2/2b}$ (see Eq.12) helps to avoid that difficulty. For this, it must be $\mathcal{N}^2 \ll |b^2|$, where $||$ denotes the modulus of a complex number.

Besides simplifying Eq.16, the $\mathcal{N}^2 \ll |b^2|$ limit also modifies Eq.17 as follows:

$$Q_{ij} = T_{ij}^{(1)}b^{-9/2} \left(b^2 + \frac{15}{8}b + \frac{105}{128} - \frac{5}{4}\mathcal{N}^2 \right) - T_{ij}^{(2)}b^{-11/2} \left(b^2 + \frac{35}{8}b + \frac{945}{128} - \frac{7}{4}\mathcal{N}^2 \right) \quad (18)$$

The limit in question is a small β_T limit which also interests \mathcal{N} and thus the refractive index components. However, here below it is shown to be less restrictive than Eq.1.

From the definitions 12-13, the inequality writes:

$$2\frac{N_{\perp}^2}{Y^2}(1 - \cos Y\tau) + N_{\parallel}^2\tau^2 \ll \frac{1}{\beta_T^4} + \tau^2 \quad (19)$$

The smallness -at any time τ - of the first term on the left hand side requires $\frac{N_{\perp}^2}{Y^2} \ll \frac{1}{\beta_T^4}$ i.e. relatively small Larmor radii ($\lambda \ll \frac{1}{\beta_T^2} <$), although not as small as in the conventional finite Larmor radius (FLR) limit ($\lambda \ll 1$). For example, for electromagnetic waves of $N_{\perp} \leq 1$, it is sufficient to meet a requirement on the magnetic field, $Y \gg \beta_T^2$, which is fulfilled in most magnetized laboratory plasmas. For Bernstein waves (reaching the highest perpendicular refractive index, $N_{\perp} \approx \frac{Y}{\beta_T}$, such that $\lambda \approx 1$) the requirement is simply $\beta_T \ll 1$, which is being assumed through this weakly relativistic treatment anyway.

The second term on the left hand side of Eq.19, $N_{\parallel}^2\tau^2$, should in principle be much smaller than the right hand side. This is always the case if $N_{\parallel} \leq 1$, at any time τ . If $N_{\parallel} > 1$ the condition is violated from time $\tau_1 = \frac{1}{\beta_T^2} \frac{1}{\sqrt{N_{\parallel}^2 - 1}}$ onwards. However, the wave-particle interaction weakens as time progresses and the decay is particularly rapid in the $N_{\parallel} > 1$ case. This is because in that case, apart from an oscillation due to the finite N_{\perp} , R is a growing function of τ , and the integrand I_{ij} of Eq.4 decays exponentially with R , as illustrated by Eq.16. To fix the ideas, the wave-particle interaction can be considered negligible when $e^{-R^{1/2}}$ reaches a thousandth of its initial value $e^{-\beta_T^{-2}}$. This occurs at $\tau_2 = \sqrt{\frac{49+14/\beta_T^2}{N_{\parallel}^2-1}}$. Therefore, it is sufficient to require the wave-particle interaction to become negligible before the condition 19 is formally violated. This translates into the condition $\tau_2 < \tau_1$, which is equivalent to $\beta_T < 0.24$, or $T_e < 30\text{keV}$. In turn, this should already be guaranteed by $\beta_T \ll 1$. More generally, the condition is $\beta_T^2 < \frac{\sqrt{2}-1}{\ln D}$. Here, to fix the ideas, strong damping was defined as damping by a factor $D=1000$.

Recapitulating, Eq.19 is valid for any N_{\parallel} , provided $\frac{N_{\perp}}{Y} \ll \frac{1}{\beta_T^2}$ and $\beta_T \ll 1$ or, equivalently, $\beta_T \ll \min\{1, \sqrt{Y/N_{\perp}}\}$. Under these circumstances $e^{-R^{1/2}} \simeq e^{-b} e^{-\mathcal{N}^2/2b}$, which simplifies the integration of Eq.4. $\frac{N_{\perp}}{Y} \ll \frac{1}{\beta_T^2}$ is indeed a FLR condition, as it may be rewritten as $\lambda \ll \frac{1}{\beta_T^2}$, but less stringent than Eq.3, as it includes higher order FLR corrections compared to $\lambda \ll 1$.

Note that Eq.19 is an independent requirement not related to Eqs.1-2, which are not invoked here. All these equations impose an upper limit to N components, although the limit scales like powers of β_T in Eqs.1-2 and like an inverse power in Eq.19. In this respect Eq.19 is more similar to the small Larmor radius condition Eq.3, but is less restrictive for N_{\perp} , thank to the weakly relativistic limit.

B. Weakly relativistic limit of the integrand in Eq.5

For an alternative derivation of Eqs.16-18, γ can be Taylor-expanded up to the second order in u in Eq.5, which takes the form:

$$I_{ij} = \frac{e^{i\tau}}{(2\pi\beta_T^2)^{3/2}(1 + \frac{15}{8}\beta_T^2)} T_{jk}^{(1)} \int d^3\mathbf{u} u_i u_k (2 - u_x^2 - u_y^2 - u_z^2) \mathcal{E}_x \mathcal{E}_y \mathcal{E}_z / 2 \quad (20)$$

where

$$\mathcal{E}_x = \exp \left[-i\mathcal{N}_x u_x + \frac{u_x^2}{2} (i\tau - \beta_T^{-2}) \right] \quad (21)$$

and equivalent definitions apply to \mathcal{E}_y and \mathcal{E}_z .

After substituting Eq.9, one can recognize in \mathcal{E}_z the term $-i\mathcal{N}_{\parallel} u_{\parallel} \tau$ responsible for Doppler broadening. The source of weakly relativistic broadening $i u^2 \tau / 2$ dominates over it if $N_{\parallel} \ll u$, but for the sake of generality and to cope with $N_{\parallel} \approx u$, both terms are retained here.

The main advantage of Eq.20 over Eq.5 is that the parallel and perpendicular degree of freedom, which were previously coupled by γ , are now decoupled. The approximation of γ^{-1} with a sum and of the exponent with a product of functions of u_x , u_y or u_z only, ease the integration over \mathbf{u} . In fact, this reduces to a sum of products of integrals of type:

$$\int_{-\infty}^{\infty} du_x e^{-i\mathcal{N}_x u_x - b u_x^2 / 2} = \sqrt{\frac{2\pi}{b}} e^{-\mathcal{N}_x^2 / 2b} \quad (22)$$

and its derivatives up to the 4th order in \mathcal{N}_x . Similar integrals in u_y and u_z , as well as their derivatives, are also involved. Note that in the integrals above the real part of b is positive. After some algebra, the same result as in Eq.16 is obtained, but with different

coefficients for Eq.18:

$$Q_{ij} = T_{ji}^{(1)} b^{-9/2} \left(b^2 - \frac{5}{2}b + \frac{\mathcal{N}^2}{2} \right) - T_{ji}^{(2)} b^{-11/2} \left(b^2 - \frac{7}{2}b + \frac{\mathcal{N}^2}{2} \right) \quad (23)$$

This is because, although physically more explicit, the second method is based on the exact integration of an approximated integrand (Eq.20). Therefore, it is only valid in the limit in which the approximated distribution and wave-particle interaction are plausible. Although not maxwellian, neither classically nor relativistically, the distribution f used in Eq.20 is correct in a semi-relativistic sense and is correctly normalized, i.e. the approximation conserves the number of particles. However, the description of the wave-particle interaction in Eq.20 is correct only at the leading orders in b . For these reasons, we will adopt for the remainder the more rigorous Eq.18, resulted from the Taylor approximation of the exact integral, Eq.11.

III. EXPANSION IN CYCLOTRON HARMONICS

First of all, it is convenient to change variables and absorb the thermal velocity in the definitions of time and cyclotron frequency:

$$t = \beta_T^2 \tau \quad y = Y/\beta_T^2. \quad (24)$$

The contributions of individual cyclotron harmonics to Eq.16 can be separated from each other by rewriting as follows a term involved in $e^{-R^{1/2}}$:

$$\exp \left[\frac{\lambda \cos yt}{1 - it} \right] = \sum_{p=0}^{\infty} \frac{1}{p!} \left[\frac{\lambda}{1 - it} \frac{e^{iyt} + e^{-iyt}}{2} \right]^p \quad (25)$$

with the double series *restricted to even values of $m + n$* .

The binomial theorem transforms Eq.25 in

$$\exp \left[\frac{\lambda \cos yt}{1 - it} \right] = \sum_{p=0}^{\infty} \sum_{q=0}^{\infty} \left[\frac{\lambda}{2(1 - it)} \right]^{p+q} \frac{e^{i(p-q)yt}}{p!q!} \quad (26)$$

Finally, considerations about how to fill the first quadrant $p > 0, q > 0$, with sums over $m = p + q$ and $n = p - q$, lead to:

$$\exp \left[\frac{\lambda \cos yt}{1 - it} \right] = \sum_{n=-\infty}^{\infty} \sum_{m=|n|}^{\infty} \left[\frac{\lambda}{2(1 - it)} \right]^m \frac{e^{inyt}}{\left(\frac{m+n}{2}\right)! \left(\frac{m-n}{2}\right)!} \quad (27)$$

With this substitution, Eqs.4 and 16 yield:

$$\epsilon_{ij} = \delta_{ij} + \frac{iX}{\beta_T^5 + \frac{15}{8}\beta_T^7} \sum_{n=-\infty}^{\infty} \sum_{m=|n|}^{\infty} \frac{(\lambda/2)^m \mathcal{Q}_{mn,ij}}{\left(\frac{m+n}{2}\right)! \left(\frac{m-n}{2}\right)!} \quad (28)$$

$$\mathcal{Q}_{mn,ij} = \int_0^\infty \frac{dt}{\beta_T^2 (1-it)^m} \exp\left[\frac{it}{\beta_T^2}(1-nY) - \frac{\lambda + N_{\parallel}^2 t^2 / 2\beta_T^2}{1-it}\right], \quad (29)$$

where, as above, the summation is *restricted to even values of $m+n$* . All integrals of type 29 can be reconducted to generalized Shkarofsky functions²⁴⁻²⁶

$$\mathcal{F}_{q,r}(z, a) = -i \int_0^\infty \frac{(it)^r}{(1-it)^q} \exp\left[izt - \frac{at^2}{1-it}\right] dt. \quad (30)$$

but of *shifted arguments* that will be omitted for brevity:

$$\mathcal{F}_{q,r} = \mathcal{F}_{q,r}(n) = \mathcal{F}_{q,r}\left(\frac{1-nY}{\beta_T^2} - \lambda, \frac{N_{\parallel}^2}{2\beta_T^2} - \lambda\right), \quad (31)$$

Unless necessary for disambiguation, also the harmonic number will be dropped. In fact, most $\mathcal{F}_{q,r}$ hereafter refer to the n -th harmonic, except for some sums and differences on side-harmonics, coincisely referred to as:

$$\mathcal{F}_{q,r}^{\pm,p} = \mathcal{F}_{q,r}(n+p) \pm \mathcal{F}_{q,r}(n-p) \quad (32)$$

Further, generalized Shkarofsky functions of $r \neq 0$ are related to standard Shkarofsky functions of $r = 0$ by derivatives or integration by parts²⁴,

$$\mathcal{F}'_q = \frac{\partial \mathcal{F}_q}{\partial z} = \mathcal{F}_{q,1} = \mathcal{F}_q - \mathcal{F}_{q-1} \quad (33)$$

$$\mathcal{F}''_q = \frac{\partial^2 \mathcal{F}_q}{\partial z^2} = \mathcal{F}_{q,2} = \mathcal{F}_q - 2\mathcal{F}_{q-1} + \mathcal{F}_{q-2}. \quad (34)$$

With these substitutions and after lengthy but straightforward calculations partly reported in appendix, one finds:

$$\mathcal{Q}_{mn,11} = iG_{mn}^+ + ia_+ \mathcal{F}_{m+\frac{9}{2}} - \frac{i N_{\perp}^2}{4 Y^2} \left[2b_l \mathcal{F}_{m+\frac{1}{2}} + b_+ \mathcal{F}_{m+\frac{11}{2}}^{\pm,1} \right] \quad (35)$$

$$\mathcal{Q}_{mn,22} = iG_{mn}^+ + ia_+ \mathcal{F}_{m+\frac{9}{2}} - i \frac{N_{\perp}^2}{Y^2} \left[b_l \left(\mathcal{F}_{m+\frac{1}{2}}^{\pm,1} - \frac{3}{2} \mathcal{F}_{m+\frac{1}{2}} \right) + b_+ \left(\mathcal{F}_{m+\frac{11}{2}}^{\pm,2} - \frac{7}{4} \mathcal{F}_{m+\frac{11}{2}}^{\pm,1} + 2\mathcal{F}_{m+\frac{11}{2}} \right) \right] \quad (36)$$

$$\mathcal{Q}_{mn,12} = G_{mn}^- - \frac{1 N_{\perp}^2}{4 Y^2} \left[2b_l \mathcal{F}_{m+\frac{9}{2}}^{\pm,1} + b_+ \left(2\mathcal{F}_{m+\frac{11}{2}}^{\pm,2} - \mathcal{F}_{m+\frac{11}{2}}^{\pm,1} \right) \right] \quad (37)$$

$$\mathcal{Q}_{mn,13} = -\frac{i N_{\perp}}{2 Y} \frac{N_{\parallel}}{\beta_T^2} \left(b_l \mathcal{F}_{m+\frac{1}{2}}^{\pm,1} + b_+ \mathcal{F}_{m+\frac{11}{2}}^{\pm,2} \right)' \quad (38)$$

$$\mathcal{Q}_{mn,23} = \frac{1 N_{\perp}}{2 Y} \frac{N_{\parallel}}{\beta_T^2} \left[b_l \left(\mathcal{F}_{m+\frac{1}{2}}^{\pm,1} - 2\mathcal{F}_{m+\frac{1}{2}} \right)' + b_+ \left(\mathcal{F}_{m+\frac{11}{2}}^{\pm,2} - 2\mathcal{F}_{m+\frac{11}{2}}^{\pm,1} + 2\mathcal{F}_{m+\frac{11}{2}} \right)' \right] \quad (39)$$

$$\mathcal{Q}_{mn,33} = i \left(a_l \mathcal{F}_{m+\frac{1}{2}} + a_+ \mathcal{F}_{m+\frac{9}{2}}^{\pm,1} \right) + i \frac{N_{\parallel}^2}{\beta_T^4} \left(b_l \mathcal{F}_{m+\frac{1}{2}} + b_+ \mathcal{F}_{m+\frac{11}{2}}^{\pm,1} \right)'' \quad (40)$$

where

$$G_{mn}^{\pm} = \frac{1}{2} \left(a_l \mathcal{F}_{m+\frac{l}{2}}^{\pm,1} + a_+ \mathcal{F}_{m+\frac{9}{2}}^{\pm,2} \right) + \frac{1}{4} \frac{N_{\perp}^2}{Y^2} \left(b_l \mathcal{F}_{m+\frac{l}{2}}^{\pm,2} + b_+ \mathcal{F}_{m+\frac{11}{2}}^{\pm,3} \right), \quad (41)$$

and $\mathcal{Q}_{mn,21} = -\mathcal{Q}_{mn,12}$, $\mathcal{Q}_{mn,31} = \mathcal{Q}_{mn,13}$, $\mathcal{Q}_{mn,32} = -\mathcal{Q}_{mn,23}$. It is worth reminding that here Shkarofsky functions $\mathcal{F}_{q,r}$ have shifted arguments like in Eq.31.

The convention of summing over repeated indices is adopted; scalar products involve the coefficients:

$$(a_5, a_7, a_9) = \frac{5}{2} e^{-\lambda} \beta_T^3 \left[\left(\frac{2}{5} + \frac{N_{\parallel}^2}{2} \right), \left(\frac{3}{4} \beta_T^2 - N_{\parallel}^2 \right), \left(\frac{N_{\parallel}^2}{2} - \lambda \beta_T^2 \right) \right] \quad (42)$$

$$(b_7, b_9, b_{11}) = \frac{7}{2} e^{-\lambda} \beta_T^5 \left[\left(\frac{2}{7} + \frac{N_{\parallel}^2}{2} \right), \left(\frac{5}{4} \beta_T^2 - N_{\parallel}^2 \right), \left(\frac{N_{\parallel}^2}{2} - \lambda \beta_T^2 \right) \right], \quad (43)$$

$$a_+ = \frac{5}{4} \lambda e^{-\lambda} \beta_T^5 \quad (44)$$

$$b_+ = \frac{7}{4} \lambda e^{-\lambda} \beta_T^7 \quad (45)$$

Components of order β_T^4 were removed from the square brackets in Eqs.42-43, but those of order β_T^2 and, for consistency, of order $\beta_T^2 \lambda$, were retained. The latter are formally of order β_T^4 . Nevertheless, they also involve N_{\perp} , and neglecting them indirectly implies a restriction on the Larmor radius parameter that actually, for Bernstein waves, can evaluate $\lambda \lesssim 1$ even when $\beta_T \ll 1$. For the sake of generality, N_{\parallel}^2 has also been retained in all the components, both when it appears along with a number of order 1, as well as with β_T^2 or $\lambda \beta_T^2$.

The λ -dependence of the revised generalized Shkarofsky functions is the sign that dispersion depends on the Larmor radius, in agreement with fully relativistic Eqs.4-5. The shift of $\mathcal{F}_{q,r}$ arguments z and a by an amount λ can be interpreted as a linear finite-Larmor-radius correction to the resonance condition (through $z = 2(nY + 1)/\beta_T^2$) and to its width in inhomogeneous plasmas, through the ratio of Doppler to relativistic width, $a = N_{\parallel}/\beta_T$. The physical meaning of $z \rightarrow z - \lambda$ is the well-known relativistic downshift of the peak z of emission/absorption, which also becomes manifest in a change of width of the emitting/absorbing layer, through $a \rightarrow a - \lambda$. Note that fully and weakly relativistic treatments slightly disagreed on the peak power deposition in some recent ITER modelling²⁷ and that the present z shift goes in the right direction to reconcile this disagreement.

IV. COMPARISON WITH OTHER DISPERSION FUNCTIONS

Table II clarifies under which conditions $\mathcal{F}_{q,r}(n)$ reduces to other semi-relativistic and classical plasma dispersion functions.

The $\lambda/(1-it) \simeq \lambda$ approximation of Eq.29 quoted in the table is equivalent to zeroing the λ shifts in Eq.31. The limit is justified under very weakly relativistic conditions, such that $t = \beta_T^2 \tau \ll 1$ for any “reasonable” τ , in the sense of Subsec.II.A.

We also note that double sums over the Shkarofsky function index m (sometimes called q or $q + 1/2$ or $p + n + 3/2$ in literature) and over the harmonic number n were already found by Airoidi¹⁵, Shkarofsky⁷ and Swanson^{10,28}.

A. Shkarofsky’s Tensor

Eqs.28 and 35-40 generalize the well-known Shkarofsky’s weakly relativistic tensor³ by linearly combining, by means of $N_{||}$ -dependent coefficients, Shkarofsky functions corrected for FLR effects. Higher β_T orders are also retained, compared to Shkarofsky’s treatment.

The original tensor³ can be obtained as follows. In the a and b coefficients (Eqs.42-45) one has to a) keep only the lowest order in β_T , b) set $e^{-\lambda} = 1$ and c) $N_{||} = 0$. Approximations b) and c) are equivalent to neglect finite Larmor radius and oblique incidence corrections, respectively. As a result, the only non-vanishing coefficients are $a_5 = \beta_T^3$ and $b_7 = \beta_T^5$. Correspondingly, only the $\mathcal{F}_{n+\frac{5}{2}}$ and $\mathcal{F}_{n+\frac{7}{2}}$ functions remain in use and Eqs.35-40 simplify as follows:

$$\mathcal{Q}_{mn,11} = \mathcal{Q}_{mn,22} = \frac{i\beta_T^3}{2} \mathcal{F}_{m+\frac{5}{2}}^{+,1} \quad (46)$$

$$\mathcal{Q}_{mn,12} = \frac{\beta_T^3}{2} \mathcal{F}_{m+\frac{5}{2}}^{-,1} \quad (47)$$

$$\mathcal{Q}_{mn,13} = -iN_{||} \frac{N_{\perp}}{Y} \frac{\beta_T^3}{2} \mathcal{F}_{m+\frac{7}{2}}^{-,1} \quad (48)$$

$$\mathcal{Q}_{mn,23} = N_{||} \frac{N_{\perp}}{Y} \frac{\beta_T^3}{2} \left(\mathcal{F}_{m+\frac{7}{2}}^{+,1} - 2\mathcal{F}'_{m+\frac{7}{2}} \right) \quad (49)$$

$$\mathcal{Q}_{mn,33} = i\beta_T^3 \mathcal{F}_{m+\frac{5}{2}} + iN_{||}^2 \beta_T \mathcal{F}_{m+\frac{7}{2}}'' \quad (50)$$

Moreover, d) the FLR parameter λ has to be zeroed in Eq.31, e) the second sum in Eq.28 has to be truncated to $m = |n|$,

$$\epsilon_{ij} = \delta_{ij} + \frac{iX}{\beta_T^5} \left[\mathcal{Q}_{00,ij} + \sum_{n=1}^{\infty} \frac{\lambda^n}{2^n n!} (\mathcal{Q}_{nn,ij} + \mathcal{Q}_{n-n,ij}) \right], \quad (51)$$

which is equivalent to truncate the Taylor expansion of Bessel functions I_n to their leading order, λ^n . Additionally, f) only the leading β_T order has to be retained at denominator in Eq.28.

Substituting Eqs.46-50 in Eq.51 returns Eqs.4a-4c of Shkarofsky³. Note that the $_{11}$ and $_{22}$ components are identical, while they differ from each other in the fully relativistic tensor¹, in the present weakly relativistic treatment (Eqs.35 and 36) and in the warm dielectric tensor²⁹, as they should in presence of finite but relativistically distorted Larmor orbits, due to the different nature of the Doppler shift (transverse or longitudinal) that breaks the cylindrical symmetry of the plasma response around the magnetic field direction.

B. Warm Tensor

It is well-known⁶ that Shkarofsky functions can be expressed in terms of the classical dispersion function Z . Under proper limits (Tab.I) they actually coincide with it, apart from a factor: at low β_T , both arguments $z = \frac{1-nY}{\beta_T^2} - \lambda$ and $a = \frac{N_{\parallel}^2}{2\beta_T^2} - \lambda$ diverge, the $-\lambda$ corrections introduced in Eq.31 become negligible and the asymptotic limit^{24,30}

$$\mathcal{F}_q(z, a) \simeq -\frac{Z(\Psi)}{\sqrt{4a+2q}} \simeq -\frac{\beta_T}{\sqrt{2}N_{\parallel}} Z(\Psi) \quad (52)$$

applies. Here

$$\Psi = \frac{z+q}{\sqrt{4a+2q}} \simeq \frac{1}{\sqrt{2}} \frac{1-nY}{N_{\parallel}\beta_T}. \quad (53)$$

On the other hand, it is easy to identify the sum over m in Eq.27 as the generating function for the modified Bessel function of the first kind:

$$\exp\left[\frac{\lambda \cos yt}{1-it}\right] = \sum_{n=-\infty}^{\infty} I_n\left(\frac{\lambda}{1-it}\right) e^{inyt} \quad (54)$$

that, for $\lambda/(1-it) \simeq \lambda$ yields a familiar portion of the warm dielectric tensor components ϵ_{11} , ϵ_{22} , ϵ_{33} , ϵ_{13} :

$$\exp\left[\frac{\lambda \cos yt}{1-it}\right] \simeq \sum_{n=-\infty}^{\infty} I_n(\lambda) e^{inyt} \quad (55)$$

To recover the other components it is useful to remember the recursive relation for the Bessel function derivative²³:

$$I'_n = I_{n+1} + nI_n/\lambda \quad (56)$$

After these simple steps the warm dielectric tensor (Eqs.10.40, 57, 58 of²⁹) is obtained.

C. Bessel Functions of complex time-dependent Larmor radius parameter

Yet another semi-relativistic formulation can be derived by inserting Eq.54, instead of Eq.27, in Eqs.4 and 16. Eq.54 generalizes a standard Bessel function identity utilized in deriving the warm non-relativistic dielectric tensor³¹. However, it does so by replacing λ with $\lambda/(1-it)$, i.e. by introducing a time dependence for I_n that cannot be factored out of the time integral anymore. The resulting expression,

$$\epsilon_{ij} = \delta_{ij} + \frac{iX}{\beta_T^5 + \frac{15}{8}\beta_T^7} \sum_{n=-\infty}^{\infty} \int_0^{\infty} \frac{dt}{\beta_T^2} Q_{ij} \exp \left[\frac{it}{\beta_T^2} (1 - nY) - \frac{\lambda + N_{\parallel}^2 t^2 / 2\beta_T^2}{1 - it} \right] I_n \left(\frac{\lambda}{1 - it} \right) \quad (57)$$

avoids the nuisance of the double sum over m and n but involves integrals more complicated than Eq.29 and is not convenient from a numerical standpoint. Actually it exceeds in complexity the initial fully relativistic Trubnikov's tensor of Eqs.4 and 11. Nevertheless, it is useful as it links the present weakly relativistic treatment to others. For example, an equation similar to Eq.57 was the starting point for the original Shkarofsky's derivation of 1966³ and for a revised, more general result of 1986⁷. While the Bessel functions were approximated to their leading order in λ in the initial derivation, the whole series of powers of λ was retained in the later work, yielding a double sum similar to Eq.28, the other sum being on the harmonic number. Also Eqs.2.3.53 and 78 of¹⁴ share interesting analogies with Eq.57 of the present article, in spite of the different method. There are also distinct differences, though, including the argument of the Bessel function, which was λ in those previous works^{3,7,14}, or the more drastic simplification of Q_{ij} , on the ground that the exponent has a bigger effect on the integral in Eq.57.

At this point it should be remembered that it is customary to treat as a constant the Lorentz factor γ in the denominator in the integrand of Eq.5 and to Taylor-expand only the factor γ in the exponent, the reason being that relativistic corrections in the denominator have a comparatively small effect on the integral. This is equivalent to approximating $Q_{ij} \simeq (T_{ij}^{(1)} 2b - T_{ij}^{(2)}) 8b^2$, which in turn leads to the loss of N_{\parallel} corrections in Eqs.35-45. Probably this was overlooked in the past due to the quasi-perpendicular hypothesis $N_{\parallel} \ll \beta_T$, which tended to neglect small- N_{\parallel} corrections when summed to or divided by (comparatively larger) β_T corrections.

V. NUMERICAL RESULTS

The double sum in Eq.28 may seem computationally expensive, but only four functions $\mathcal{F}_{m+\frac{l}{2}}$, with $l = 5, 7, 9$ and 11 , are used at each step m and only two of them need to be calculated. The other two can be recursively generated by^{6,24}:

$$\frac{N_{\parallel}^2}{\beta_T^2} \mathcal{F}_{m+\frac{5}{2}}(n) = 1 + \frac{2}{\beta_T^2} (N_{\parallel}^2 - 1 + mY) \mathcal{F}_{m+\frac{1}{2}}(n) - (m + \frac{1}{2}) \mathcal{F}_{m+\frac{3}{2}}(n) \quad (58)$$

The same relation also provides the functions for the following step, $m + 1$, and so on. Hence, multiple values of m in the sum of Eq.28 do not require significant extra calculations compared to the single value, $m = |n|$ case of Shkarofsky³.

The sum over n doesn't introduce significant calculations either, because the generic step n involves functions that are either known from steps $n - 1$ and $n - 2$, or will be reutilized for the $n+1$ - and $n+2$ -th harmonic. Furthermore, unless β_T and/or N_{\parallel} are high enough to cause significant harmonic overlap, i.e. if the electron cyclotron lines, although broadened, are still well-resolved, the double sum can be restricted to few values of n or just to the dominant harmonic.

The index m can also be kept small, similar to $k \leq 3$ of Swanson's moderately relativistic dielectric tensor²⁸: $m=2$ is typically a good compromise between accuracy and rapidity of calculation.

Two applications are considered in the following Subsections, to illustrate the advantages of Eq.28 over the cold and warm dielectric tensor²⁹ as well as the semi-relativistic formulations by Shkarofsky³ and Airoidi-Orefice¹⁵. To author's knowledge, the latter is computed for the first time in its generality: even the original article, despite the generality of the analytical derivation, treated numerically only a simplified case, virtually coincident with Shkarofsky's tensor. The models are compared with each other and with Trubnikov's tensor¹ (from which they all descend, after various approximations), which is taken as a reference.

A. OXB Mode Conversion

An interesting application for the new tensor is represented by the dispersion relation $\det(N_i N_j - N^2 \delta_{ij} + \epsilon_{ij}) = 0$ for an optimal value of the parallel refractive index, $N_{\parallel} = \sqrt{Y/(Y+1)}$, enabling the ordinary (O)-extraordinary (X)-Bernstein (B) mode conversion³².

For heating or emission measurements at a low harmonic ($\omega = n\omega_c$, with $n=1-5$), the optimal parallel component for the mode conversion takes values $N_{\parallel} \simeq 0.4-0.7$. These are incompatible with quasi-perpendicular incidence ($N_{\parallel} \ll \beta_T$, Eq.1) and thus not adequately modelled by Shkarofsky's and other mild relativistic formulas, and constitute a good testbed for the new results. A slab geometry is considered for simplicity. Note, however, that in more realistic geometries N_{\parallel} tends to grow even larger than the initial $N_{\parallel} \simeq 0.4-0.7$, as a result of the large N_{\perp} being projected in a curved magnetic field. This represents an additional argumentation in favor of weakly relativistic formulas valid for arbitrary N_{\parallel} .

The dispersion relation was calculated for optimal launch in a uniformly magnetized plasma ($Y=0.9$) of inhomogeneous density X . The contours corresponding to $\det(N_i N_j - N^2 \delta_{ij} + \epsilon_{ij}) = 0$ are plotted in Figs.1-5, for different temperature regimes. Although the root finder searched for N_{\perp}^2 roots, is plotted on the vertical axis, to magnify the mode conversion region at relatively low N_{\perp} .

The models examined in Figs.1-5 offer the advantage, over *electrostatic* approximations¹¹⁻¹³, of dealing simultaneously with the *electromagnetic* O- and X-mode as well as with the *electrostatic* Bernstein (B) mode.

Apart from the cold dispersion, which does not account for the Bernstein mode and for its generation at the upper hybrid resonance (UHR), and the Shkarofsky tensor, which tends to overestimate N_{\perp} for the B-mode, all the tensors considered are all also very general with respect to N_{\perp} , at least at non-relativistic temperatures: in Fig.1, N_{\perp} ranges from $N_{\perp} = 0$ at the OX mode conversion, for which the cold dielectric tensor would be sufficient, to $N_{\perp} > 1$ at the XB mode conversion, where FLR effects play a fundamental role and the warm dielectric tensor becomes necessary, up to $N_{\perp} \approx 1/\beta_T \gg 1$, for the Bernstein mode.

Most models, including the new one, agree with the fully relativistic reference up to fairly large N_{\perp} , but the warm plasma tensor shows good agreement over the broadest domain and yet it is the most economical in terms of computational resources. This confirms the appropriateness of adopting the warm tensor to trace OXB mode-converted Electron Bernstein Waves (EBWs) in plasmas of 1keV or less¹⁸.

At higher temperatures ($\beta_T=0.1$) relativistic effects start to become important and only two tensors (the warm one, and the new one presented here) show good agreement with the fully relativistic curve (Fig.2).

Relativistic corrections clearly become important at $\beta_T=0.2$, corresponding to

$T_e = 20.5\text{keV}$, as it is evident from the difference between the fully relativistic and the classical 'warm' curve in Fig.3. The new tensor best approximates Trubnikov's results (Fig.3) and it remains the best approximation at up to $\beta_T = 0.5$ ($T_e = 128\text{keV}$, Fig.4). The first significant discrepancies are encountered at $\beta_T = 0.6$ (Fig.5), and can be explained with both the $\beta_T \ll 1$ and $\frac{N_\perp}{Y} \ll \frac{1}{\beta_T^2}$ limits being violated. The latter translates in $N_\perp \ll 2.5$ in the case of interest, and is responsible for the change of slope at $N_\perp \simeq 1.2$.

It is evident from the vertical axes of Figs.1-5 that for EBWs N_\perp scales as $1/\beta_T^{33}$. In the light of this, the inequality $\frac{N_\perp}{Y} \ll \frac{1}{\beta_T^2}$ rewrites $\beta_T \ll Y$, which in fact is violated in Fig.5.

Finally, note that relativistic effects act in the correct direction, of reducing the perpendicular phase velocity c/N_\perp with respect to warm plasma calculations. This is in agreement with the relativistically increased mass and the consequent reduced thermal velocity of electrons, compared to a classical calculation for the same temperature.

Fig.6a shows a detail of Fig.3 -although with N_\perp^2 , rather than N_\perp , on the vertical axis- in the vicinity of the OX mode conversion: the O-mode branch comes from low densities and connects to the SX-mode branch at the cutoff density. Two main conclusions can be drawn from this plot.

First of all, the weakly and fully relativistic O-mode penetrates deeper than the cold and warm one. This is in agreement with the mass increase and consequent reduction of the effective plasma frequency, so that the condition $\omega = \omega_{p,rel}$, where ω is the wave frequency and $\omega_{p,rel}$ the relativistically corrected plasma frequency is achieved at slightly higher (normalized) density $X = \omega_p/\omega$, i.e. deeper in the plasma³⁴.

Secondly, although all drawn for the nominal optimal $N_{||}$, some curves access the evanescent, $N_\perp^2 < 0$ half-plane, indicating an incomplete mode conversion, subject to losses. Slightly different $N_{||}$ settings are necessary for these curves to fully develop in the $N_\perp^2 \geq 0$ half-plane, without accessing the evanescent region (Fig.6b). In other words, different tensors predict different optimal angles for the OX mode conversion, with variations as large as $\pm 2^\circ$ for $\beta_T = 0.2$. The fully relativistic calculation, which is the most reliable, confirms the cold estimate $N_{||} = \sqrt{Y/(Y+1)}$ to be optimal. This is not surprising because the cold tensor contains the basic physical ingredients for the mode conversion, and relativistic corrections displace both the O- and the X-mode cutoff density by the same amount: although for the same $N_{||}$, for $\beta_T = 0.2$ the conversion takes place at $X = 1.05$ rather than at $X = 1$.

The new tensor exhibits the best agreement with Trubnikov's reference curve, both with

respect to the optimal N_{\parallel} and to the cutoff density X .

B. Power absorption for oblique incidence

Here the absorption of electromagnetic waves polarized in the O-mode is studied for various angles of incidence on the fundamental cyclotron resonance, in a moderately relativistic regime ($\beta_T = 0.15$).

The absorption coefficient α , defined as the fractional power loss dP/P per unit length ds along the ray ($dP/P = \alpha ds$), is given by¹⁴:

$$\alpha = 2 \frac{E_i^* \epsilon_{ij}^a E_j}{\left| E_i^* \frac{\partial \Lambda_{ij}^h}{\partial \mathbf{k}} E_j \right|} \quad (59)$$

where the superscripts h and a denote respectively the hermitian and anti-hermitian part, E^* is the complex conjugate of the electric field E (polarized in the O-mode, in this case) and

$$\Lambda_{ij} = \epsilon_{ij} + N_i N_j - N^2 \delta_{ij}. \quad (60)$$

The absorption coefficient is plotted in Figs.7-9a for a mildly relativistic case ($\beta_T = 0.15$), for three values of N_{\parallel} , ranging from quasi-perpendicular incidence (dominated by relativistic broadening) to oblique incidence (with significant Doppler broadening). The coefficient α is expressed in units of vacuum wavelength λ_0 .

The optical depth $\tau = \int_0^s \alpha(s') ds'$ is also presented in dimensionless units, in Figs.7-9b, in terms of λ_0 and of the lengthscale R_0 for the inhomogeneity of the magnetic field, $Y = R_0/R$, where R is a spatial distance.

The third plot in Figs.7-9 shows the absorption shape factor $\alpha e^{-\tau}$, giving the shape of the deposition profile. It should be emphasized that Figs.7-9 refer to a single ray in a slab, hence the deposition width might be underestimated compared to experiments or to more sophisticated modelling of a beam or bundle of rays in a realistic geometry. The main purpose of these plots is to compare various absorption models under the assumptions $R_0=1\text{m}$ and $\lambda_0=2\text{mm}$.

The absorption curves obtained with the new tensor agree with other weakly relativistic approximations, in particular with Shkarofsky's, at small-to-intermediate parallel refractive indices, $N_{\parallel} \leq \beta_T$ and show the best agreement with Trubnikov's fully relativistic absorption

profiles for large angles of propagation relative to the magnetic field, such that $N_{\parallel} > \beta_T$. This is best exemplified by the optical depth τ in Fig.9b. Potential applications include problems requiring the power localization to be so accurate that small differences between the weakly and fully relativistic predictions do matter, as in the stabilization of neoclassical tearing modes in ITER²⁷.

C. Computational time

Table III summarizes the time necessary for calculating the curves in Fig.3 for the choice of parameter shown.

Evaluating the new tensor was slightly slower than computing Shkarofsky's tensor, but orders of magnitude faster than the fully relativistic treatment. This may be convenient for massive repetitive calculations: the curves in question feature only 10000 points each, but the dielectric tensor may need to be evaluated up to 10^8 times in tracing 1-10 bundles of 10-100 rays, modelled by up to 10000 points each (their spacing being smaller than the plasma size and the plasma inhomogeneity length-scale, but large compared to the wavelength, which for large refractive indices can become very small). Such an estimate also takes into account that the tensor may need to be evaluated ~ 10 times for each spatial step, for example if a 4-5th order Runge-Kutta time-advance scheme is adopted, and derivatives are needed, which in turn require the tensor to be evaluated in displaced points.

The scaling of the computational time with the parameters is also reported in Table III, allowing extrapolations to different parameter settings. The accuracy of the results depends in a more complicated manner upon the parameter settings. However, although the considered expressions formally involve infinite sums, it was empirically found that small truncation indices are generally sufficient. On the other hand modest improvements, and at higher and higher computational costs, are registered if the parameters are set to values larger or much larger than those in Table III.

The original notations have been preserved throughout the table. Most parameters, like k_{max} and m , are truncation indices for power series (finite Larmor radius expansions) or, like q_{max} and n , for sums over Shkarofsky or Bessel functions (cyclotron harmonic expansions). In the slightly more complicated expression of Ref.¹⁵, σ and its combinatorics decompositions control the approximation of the exponent; m is an index for a generalized Shkarofsky

function of $q=0$ and $r \neq 0$, expanded in Gamma-functions and binomials; k is a truncating index for the expansion of the Bessel functions in the FLR parameter; n is the harmonic number; j and L are relevant to two binomial expansions operated in the referenced article.

The integral in the second formula by Trubnikov¹, reported for convenience in Eqs.4, 11, was numerically integrated. In principle the domain of integration extends from $\tau=0$ to $\tau=\infty$, but 400 gyroperiods were retained for the numerical integration and discretized in $n_\tau=20000$ intervals to study the dispersion (Subsec.V A), while 800 gyroperiods discretized in $n_\tau=80000$ steps were used to study the absorption (Subsec.V B). The finer resolution was necessary to avoid unphysically multi-peaked deposition profiles.

Finally, high Shkarofsky function indices q are needed, in general, in order to accurately model the dispersion and absorption at large N_\perp , but the new tensor converges more rapidly in m . Yet, with $m=2$, it reproduces Trubnikov's results better than Shkarofsky does for $q = 7/2$, which corresponds to $m=3$.

VI. SUMMARY AND CONCLUSIONS

In summary a novel formulation of the semi-relativistic dielectric tensor, Eq.28, was derived in the present article in the form of a power series in the Larmor radius parameter λ , converging for any perpendicular refractive index $N_\perp \ll Y/\beta_T^2$, of a strictly weakly relativistic approximation ($\beta_T \ll 1$).

Its generality and complexity are intermediate between Trubnikov's fully relativistic tensor and Shkarofsky's weakly relativistic tensor, in that it is also weakly relativistic, but does not contain approximations on $a = N_\parallel/\beta_T$ nor on the Larmor radius parameter λ , except for those which indirectly follow from $\beta_T \ll 1$ and from the factorization of an exponent in the time integral, based on the relatively benign request of Eq.19.

The new tensor describes the propagation (including electrostatic propagation based on finite Larmor radius effects) and damping (corrected for relativistic effects and Doppler broadening) of modes of arbitrary wavenumbers and orientation relative to the magnetic field, including the Bernstein mode. The new tensor was tested in and applied to calculations of Doppler and relativistic broadening as well as in the dispersion relation for the OXB mode conversion.

Acknowledgments

The author thanks N.Marushchenko and R.Prater for the encouragement and the stimulating discussions.

APPENDIX: DERIVATION OF EQS.35-40

In order to identify $\mathcal{F}_{q,r}$ functions in Eq.29, it is useful to define two operators in analogy with $T^{(1)}$ and $T^{(2)}$ of Eqs.6, 14:

$$\mathcal{T}^{(1)} = \begin{pmatrix} C & -S & 0 \\ S & C & 0 \\ 0 & 0 & I \end{pmatrix} \quad (\text{A.1})$$

$$\mathcal{T}^{(2)} = \frac{1}{Y^2} \begin{pmatrix} N_{\perp}^2 S^2 & N_{\perp}^2 S(C-1) & N_{\perp} N_{\parallel} S L \\ -N_{\perp}^2 S(C-1) & -N_{\perp}^2 (C-1)^2 & -N_{\perp} N_{\parallel} (C-1)L \\ N_{\perp} N_{\parallel} S L & N_{\perp} N_{\parallel} (C-1)L & N_{\parallel}^2 L^2 \end{pmatrix} \quad (\text{A.2})$$

These are indeed matrices of operators. The individual operators are C , S , L and I . They act on an integral by multiplying its integrand by, respectively, $\cos yt$, $\sin yt$, yt or 1. Their effect on generalized Shkarofsky functions is simply to change the harmonic number n or the index r :

$$C\mathcal{F}_{q,r} = [\mathcal{F}_{q,r}(n+1) + \mathcal{F}_{q,r}(n-1)]/2 = \mathcal{F}_{q,r}^{+,1}/2 \quad (\text{A.3})$$

$$S\mathcal{F}_{q,r} = [-\mathcal{F}_{q,r}(n+1) + \mathcal{F}_{q,r}(n-1)]/2i = -\mathcal{F}_{q,r}^{-,1}/2i \quad (\text{A.4})$$

$$L\mathcal{F}_{q,r} = -iy \mathcal{F}_{q,r+1} \quad (\text{A.5})$$

$$I\mathcal{F}_{q,r} = \mathcal{F}_{q,r} \quad (\text{A.6})$$

Here, when the argument n is dropped, it is understood that $\mathcal{F}_{q,r}$ refers to the n -th harmonic. The apices in Eqs.A.3-A.4 denote a sum or difference of Shkarofsky functions, according to Eq.32. Finally, the $r = 0$ case of Eq.A.5 is, according to Eq.33,

$$L\mathcal{F}_q = -iy \mathcal{F}_{q,1} = -iy(\mathcal{F}_q - \mathcal{F}_{q-1}) = -iy\mathcal{F}'_q \quad (\text{A.7})$$

The new operators allow to handle the numerous integrals of type 29 and to obtain or recognize a new integral by applying an operator (i.e., changing the indices) to an old

one. With this approach, all integrals descend from one. This initial integral, $i\frac{e^{-\lambda}}{\beta_T^2}\mathcal{F}_{m,0}$, is obtained from Eq.29 for $Q_{ij} = 1$. Following the scheme of Eqs.18 it is easy to combine the above operators into another one, that multiplies integrands by Q_{ij} . Then Eq.29 becomes:

$$\begin{aligned} \mathcal{Q}_{mn,ij} = & ie^{-\lambda} \beta_T^3 \mathcal{T}_{ij}^{(1)} \left[\mathcal{F}_{m+\frac{5}{2}} + \frac{15}{8}\beta_T^2 \mathcal{F}_{m+\frac{7}{2}} + \frac{5}{4}N_{\parallel}^2 \mathcal{F}_{m+\frac{9}{2},2} - \frac{5}{4}\beta_T^2 \lambda \left(2\mathcal{F}_{m+\frac{9}{2}} - \mathcal{F}_{m+\frac{9}{2}}^{+,1} \right) \right] \text{A.8)} \\ & - ie^{-\lambda} \beta_T^5 \mathcal{T}_{ij}^{(2)} \left[\mathcal{F}_{m+\frac{7}{2}} + \frac{35}{8}\beta_T^2 \mathcal{F}_{m+\frac{9}{2}} + \frac{7}{4}N_{\parallel}^2 \mathcal{F}_{m+\frac{11}{2},2} - \frac{7}{4}\beta_T^2 \lambda \left(2\mathcal{F}_{m+\frac{11}{2}} - \mathcal{F}_{m+\frac{11}{2}}^{+,1} \right) \right] \text{A.9)} \end{aligned}$$

This contains some generalized functions, $\mathcal{F}_{m+\frac{9}{2},2}$ and $\mathcal{F}_{m+\frac{11}{2},2}$, that can be reconducted to simple Shkarofsky functions of $r = 0$ by integrating by parts (Eq.34):

$$\mathcal{Q}_{mn,ij} = i\mathcal{T}_{ij}^{(1)} \left(a_l \mathcal{F}_{m+\frac{l}{2}} + a_+ \mathcal{F}_{m+\frac{9}{2}}^{+,1} \right) - i\mathcal{T}_{ij}^{(2)} \left(b_l \mathcal{F}_{m+\frac{l}{2}} + b_+ \mathcal{F}_{m+\frac{11}{2}}^{+,1} \right) \quad (\text{A.10})$$

where the convention of summing over repeated indices is adopted and the coefficients a and b were given in Eqs.42-45.

Applying $\mathcal{T}^{(1)}$ and $\mathcal{T}^{(2)}$ does not rise the index $r = 0$ of the $\mathcal{F}_{q,r}$ functions in Eq.A.10, because neither of the operators that they contain acts on r (see Eqs.A.3, A.4 and A.7)³⁷.

Also, they don't introduce any new explicit dependence on β_T .

At this point $\mathcal{T}_{ij}^{(1)}$ and $\mathcal{T}_{ij}^{(2)}$ should be detailed according to Eqs.A.1-A.2. For instance, for the first component,

$$\mathcal{Q}_{mn,11} = iC \left(a_l \mathcal{F}_{m+\frac{l}{2}} + a_+ \mathcal{F}_{m+\frac{9}{2}}^{+,1} \right) - i\frac{N_{\perp}^2}{Y^2} S^2 \left(b_l \mathcal{F}_{m+\frac{l}{2}} + b_+ \mathcal{F}_{m+\frac{11}{2}}^{+,1} \right) \quad (\text{A.11})$$

Following the rules for C (Eq.A.3) and S (Eq.A.4), the result Eq.35 is found. The same procedure can be used for the other components, leading to Eqs.36-40.

-
- * volpe@fusion.gat.com; Present address: General Atomics, San Diego, CA, U.S.A.
- ¹ B. A. Trubnikov, in *Plasma Physics and the Problem of Controlled Thermonuclear Reactions* (Pergamon Press, New York, 1959), vol. III, p. 122.
 - ² Y. N. Dnestrovskii, D. P. Kostomarov, and N. V. Skrydlov, *Sov. Phys.-Tech. Phys.* **8**, 691 (1964).
 - ³ I. P. Shkarofsky, *Phys. Fluids* **9**, 561 (1966).
 - ⁴ P. A. Robinson, *J. Plasma Phys.* **37**, 435 (1987).
 - ⁵ P. A. Robinson, *J. Plasma Phys.* **37**, 449 (1987).
 - ⁶ V. Krivenski and A. Orefice, *J. Plasma Phys.* **30**, 125 (1983).
 - ⁷ I. P. Shkarofsky, *J. Plasma Phys.* **35**, 319 (1986).
 - ⁸ P. H. Yoon and R. C. Davidson, *J. Plasma Phys.* **43**, 269 (1990).
 - ⁹ P. A. Robinson, *Phys. Fluids* **31**, 107 (1988).
 - ¹⁰ D. G. Swanson, *Plasma Phys. Control. Fusion* **44**, 1329 (2002).
 - ¹¹ A. N. Saveliev, *Plasma Phys. Control. Fusion* **47**, 2003 (2005).
 - ¹² A. D. Piliya, A. Y. Popov, and E. N. Tregubova, *Plasma Phys. Control. Fusion* **45**, 1309 (2003).
 - ¹³ E. Lazzaro and A. Orefice, *Phys. Fluids* **23**, 2330 (1980).
 - ¹⁴ M. Bornatici, R. Cano, O. D. Barbieri, and F. Engelmann, *Nucl. Fusion* **23**, 1153 (1983), sec.2.3.
 - ¹⁵ A. C. Airoidi and A. Orefice, *J. Plasma Phys.* **27**, 515 (1982).
 - ¹⁶ H. P. Laqua, V. Erckmann, H. J. Hartfuß, H. Laqua, W.-A. Team, and E. Group, *Phys. Rev. Lett.* **78**, 3467 (1997).
 - ¹⁷ H. P. Laqua, H. J. Hartfuß, and W.-A. Team, *Phys. Rev. Lett.* **81**, 2060 (1998).
 - ¹⁸ F. Volpe and H. P. Laqua, *Rev. Sci. Instrum.* **74**, 1409 (2003).
 - ¹⁹ H. P. Laqua, H. Maassberg, N. B. Marushchenko, F. Volpe, A. Weller, W.-A. Team, W. Kasparek, and E. Group, *Phys. Rev. Lett.* **90**, 75003 (2003).
 - ²⁰ C. B. Forest, P. K. Chattopadhyay, R. W. Harvey, and A. P. Smirnov, *Phys. Plasmas* **7**, 1352 (2001).
 - ²¹ D. W. Ignat and M. W. Ono, *Phys. Plasmas* **2**, 1899 (1995).
 - ²² E. Mazzucato, *Phys. Fluids B* **4**, 3460 (1992).
 - ²³ M. Abramowitz and I. A. Stegun, *Handbook of Mathematical Functions* (Dover Publications,

- New York, 1974), pp.374-379.
- ²⁴ P. A. Robinson, *J. Math. Phys.* **27**, 1206 (1986).
- ²⁵ N. M. Temme, A. E. Sumner, and S. S. Sazhin, *Astrophys. and Space Sc.* **194**, 173 (1992).
- ²⁶ D. B. Melrose (2006), private communication.
- ²⁷ W.A.Houlberg, C.Gormezano, J.F.Artaud, E.Barbato, V.Basiuk, A.Becoulet, P.Bonoli, R.V.Budny, L.G.Eriksson, D.Farina, et al., *Nucl. Fusion* **45**, 1309 (2005).
- ²⁸ D. G. Swanson, *Plasma Waves, 2nd Edition* (Institute of Physics Publishing, Bristol and Philadelphia, 2003), pp.205-207.
- ²⁹ T. H. Stix, *Waves in Plasmas* (AIP, New York, 1992), pp.7-9 and 252-258.
- ³⁰ C. Maroli and V. Petrillo, *Physica Scripta* **24**, 955 (1981).
- ³¹ M. Brambilla, *Kinetic Theory of Plasma Waves - Homogeneous Plasmas* (Oxford Univ.Press, 1998), p.155.
- ³² J. Preinhaelter and V. Kopecký, *J. Plasma Phys.* **10**, 1 (1973).
- ³³ F. Volpe, Ph.D. thesis, EMAU University Greifswald (2003).
- ³⁴ S. Pešić and L. Nikolić, *Plasma Phys. Control. Fusion* **41**, L49 (1999).
- ³⁵ B. D. Fried and S. D. Conte, *The Plasma Dispersion Function* (Academic Press, New York, 1961).
- ³⁶ Similar to Eqs.2.3.23 and 2.3.75-76 and to Eqs.2.3.35 and 2.3.76-77 of Ref.¹⁴, respectively. $|N_{\parallel}| \ll 1$ is needed, according to Ref.¹⁴, for the second treatment to be valid and equivalent to the first one.
- ³⁷ Actually in general L does act on r (Eq.A.5), but its effect on $r = 0$ is the same as deriving with respect to z (Eq.A.7).

TABLES

TABLE I: Summary of approximations on N_{\parallel} and λ in available weakly relativistic dielectric tensors. Some power series are truncated (trunc.). Some N_{\parallel} approximations and asymptotic developments for $\lambda \gg 1$ are accompanied by an electrostatic (e.s.) approximation.

	$\lambda \ll 1$	$\lambda \ll 1$	$\lambda \gg 1$	$\lambda \gg 1$
	trunc.			trunc.
$N_{\parallel} = 0$	4,5			
$N_{\parallel} \ll \beta_T$	3,6	7-10,28	¹² (e.s.), ⁸	¹³ (e.s.)
arbitr. N_{\parallel}		15	¹¹ (e.s.)	

TABLE II: Classical and weakly relativistic plasma dispersion functions

Approximations	Function	Ref.
none	$\mathcal{F}_{q,r}(n)$	Eq.31
$\lambda/(1-it) \simeq \lambda$	generaliz. Shkarofsky $\mathcal{F}_{q,r}(z, a)$	24
$\lambda/(1-it) \simeq \lambda, r = 0$	Shkarofsky functions $\mathcal{F}_q(z)$	3
$\lambda/(1-it) \simeq \lambda, r = 0, a = 0$	Dnestrovskii functions F_q	2
$\lambda/(1-it) \simeq \lambda, r = 0, z = 0$	plasma disp. function $Z(\zeta)$	35

TABLE III: Time required for computing the dielectric tensor 10000 times on a 1.6GHz AMD Sempron processor, for various relativistic, weakly relativistic and classical models (see Fig.1)

Model	Parameters	CPU time t (s)	scaling
cold ²⁹		0.304	
warm ²⁹	nr. Bessel functions $n=2$	0.447	$t \propto n$
Shkarofsky ³	$q_{max} = \frac{7}{2}$	2.020	$t \propto (q_{max} - \frac{1}{2})$
Airoidi-Orefice ¹⁵	$k_{max} = 3, L_{max} = 3, \sigma_{max} = 3, n = 2$	227.520	$t \propto k_{max}L_{max}\sigma_{max}n$
Volpe	$m = 3, n = 2$	2.181	$t \propto mn$
2nd Trubnikov ¹	nr. steps in integral, $n_\tau = 20000$	3689.200	$t \propto n_\tau$

FIGURE CAPTIONS

FIG.1 (color online) (a) Dispersion relation for OXB mode conversion for $Y = \omega_c/\omega=0.9$, optimal $N_{\parallel} = \sqrt{Y/(Y + 1)}$ and a moderate electron thermal velocity $\beta_T = v_T/c=0.05$, according to various relativistic, weakly relativistic and classical dielectric tensors. $X = \omega_p/\omega$ is the normalized density. (b) Detail of Fig.1.a for low N_{\perp} , showing the fast eXtraordinary (FX) branch of the dispersion relation, the Ordinary (O) one converting into the slow eXtraordinary (SX) which is attracted by the Upper Hybrid Resonance (UHR) and eventually (Fig.1a) converts into the Bernstein (B) mode.

FIG.2 (color online) Like Fig.1a, for $\beta_T=0.1$.

FIG.3 (color online) Like Fig.1a, for $\beta_T=0.2$.

FIG.4 (color online) Like Fig.1a, for $\beta_T=0.5$.

FIG.5 (color online) Like Fig.1a, for $\beta_T=0.6$.

FIG.6 (color online) Detail of the dispersion relation for $Y=0.9$ and $\beta_T=0.2$ showing the OX mode conversion for (a) $N_{\parallel} = \sqrt{Y/(Y + 1)}=0.688$ and (b) N_{\parallel} individually optimized for each dielectric tensor.

FIG.7 (color online) (a) Absorption coefficient and (b) optical depth in dimensionless units and (c) absorption shape factor for $\beta_T=0.15$ and quasi-perpendicular incidence ($N_{\parallel}=0.05$) of O-mode on fundamental electron cyclotron harmonic. $R_0=1\text{m}$, $\lambda_0=2\text{mm}$, $X=0.5$.

FIG.8 (color online) Like Fig.7, except $N_{\parallel}=0.15$.

FIG.9 (color online) Like Fig.7, but for $N_{\parallel}=0.45$, making Doppler broadening important. Note the expanded horizontal scale in Fig.c.

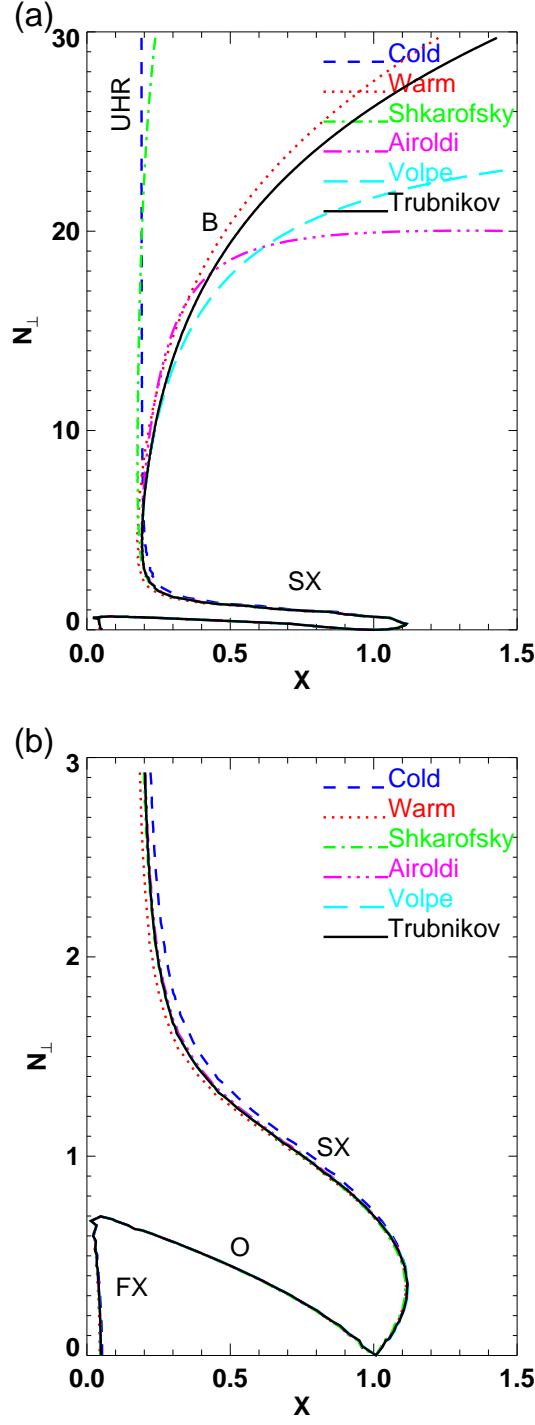


FIG. 1: (color online) (a) Dispersion relation for OXB mode conversion for $Y = \omega_c/\omega=0.9$, optimal $N_{\parallel} = \sqrt{Y/(Y+1)}$ and a moderate electron thermal velocity $\beta_T = v_T/c=0.05$, according to various relativistic, weakly relativistic and classical dielectric tensors. $X = \omega_p/\omega$ is the normalized density. (b) Detail of Fig.1.a for low N_{\perp} , showing the fast eXtraordinary (FX) branch of the dispersion relation, the Ordinary (O) one converting into the slow eXtraordinary (SX) which is attracted by the Upper Hybrid Resonance (UHR) and eventually (Fig.1a) converts into the Bernstein (B) mode.

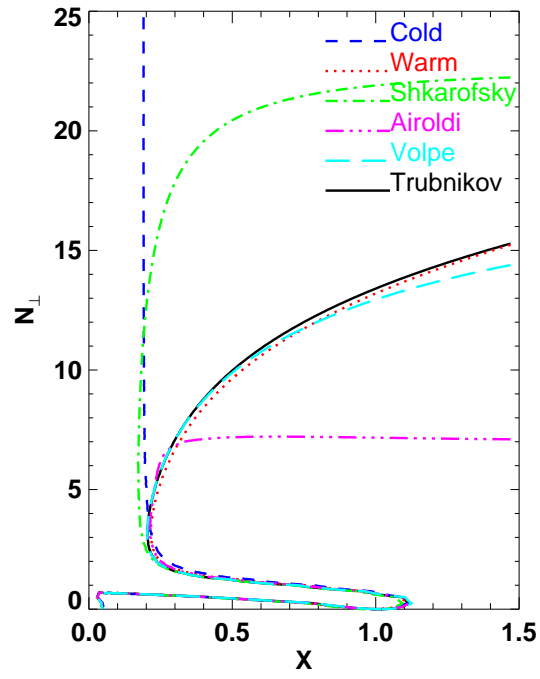


FIG. 2: (color online) Like Fig.1a, for $\beta_T=0.1$.

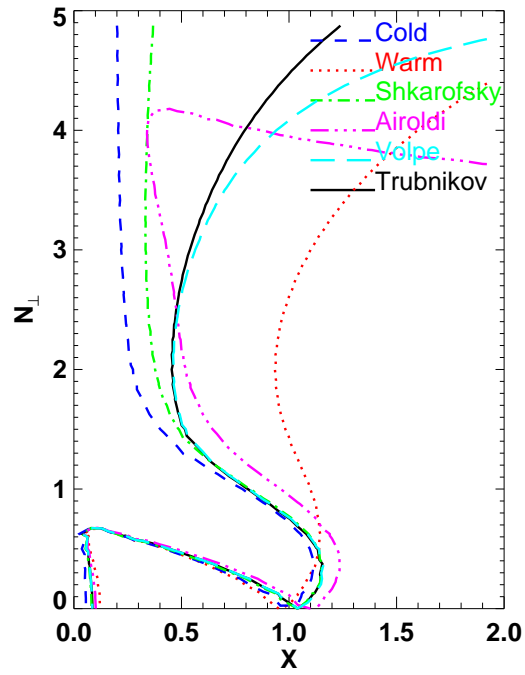


FIG. 3: (color online) Like Fig.1a, for $\beta_T=0.2$.

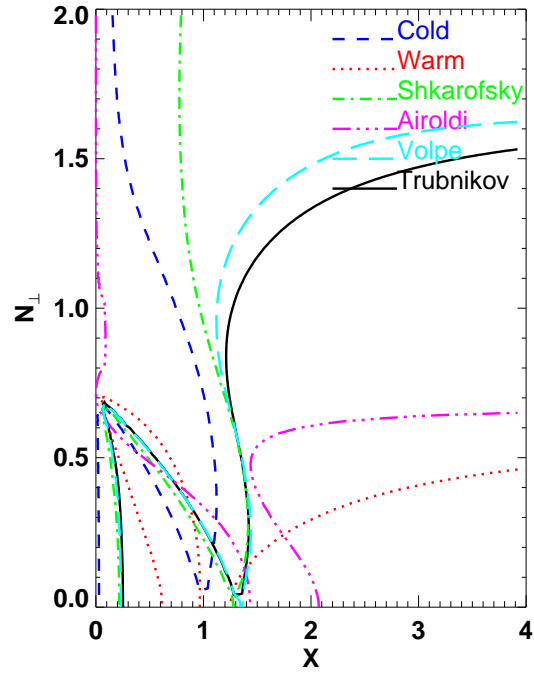


FIG. 4: (color online) Like Fig.1a, for $\beta_T=0.5$.

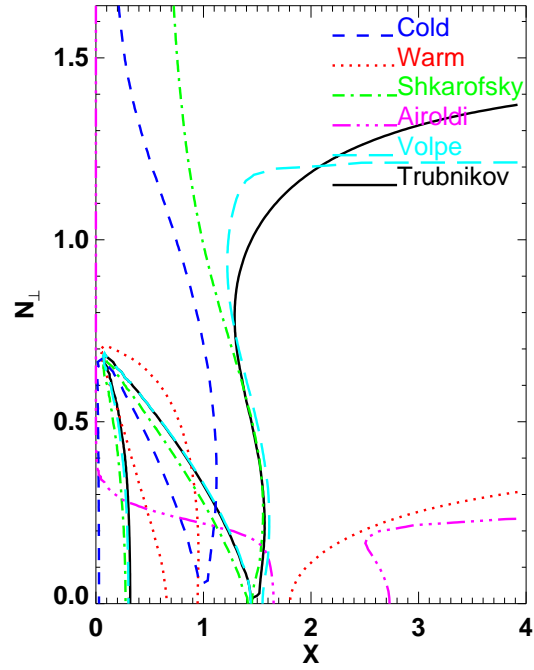


FIG. 5: (color online) Like Fig.1a, for $\beta_T=0.6$.

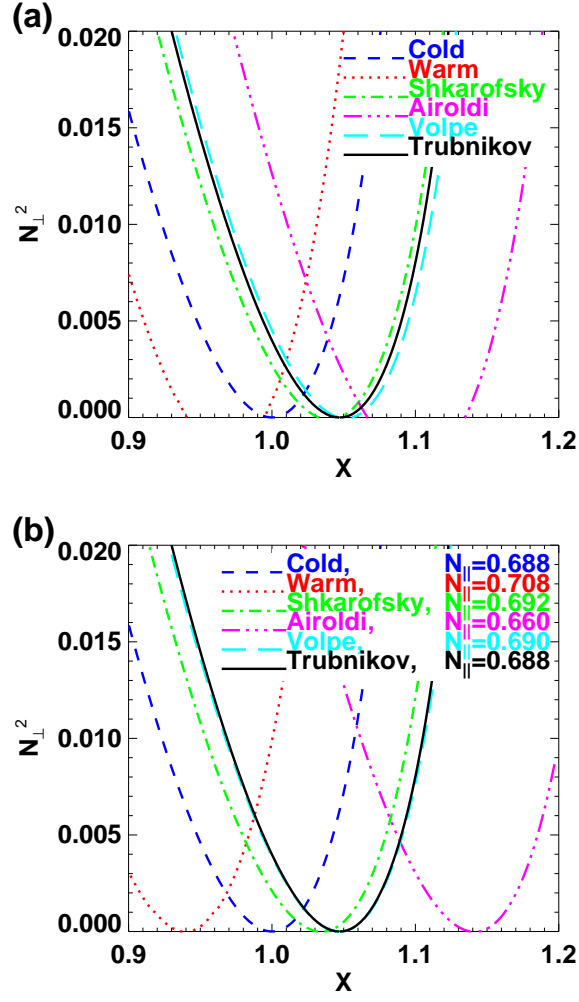


FIG. 6: (color online) Detail of the dispersion relation for $Y=0.9$ and $\beta_T=0.2$ showing the OX mode conversion for (a) $N_{\parallel} = \sqrt{Y/(Y+1)}=0.688$ and (b) N_{\parallel} individually optimized for each dielectric tensor.

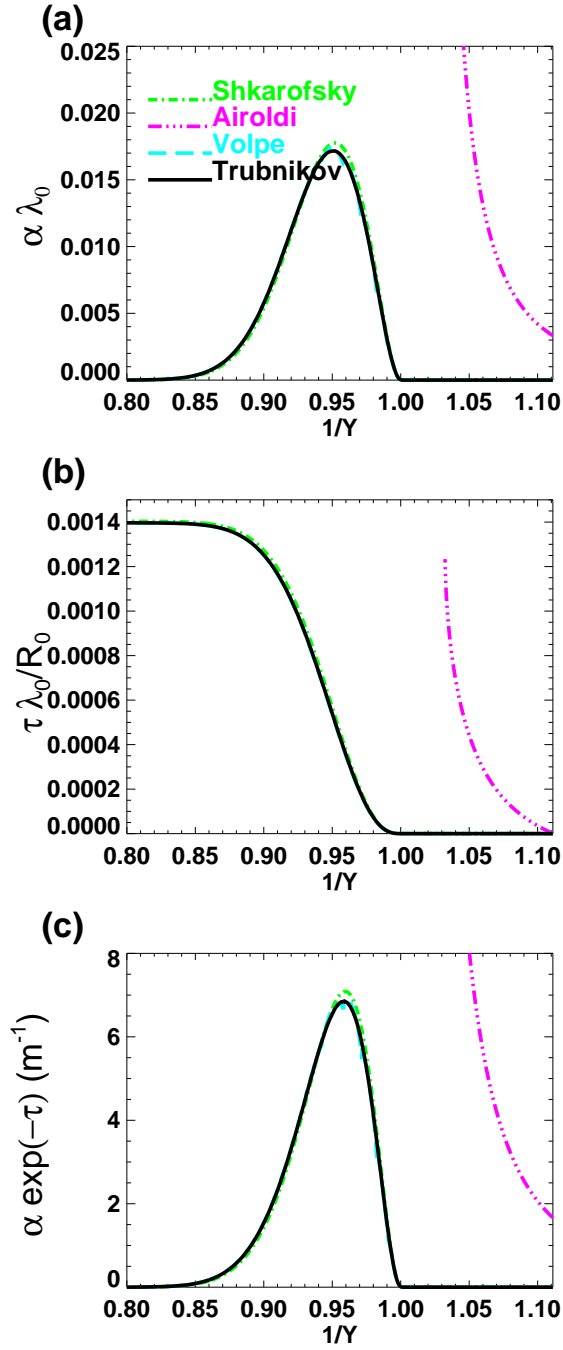


FIG. 7: (color online) (a) Absorption coefficient and (b) optical depth in dimensionless units and (c) absorption shape factor for $\beta_T=0.15$ and quasi-perpendicular incidence ($N_{\parallel}=0.05$) of O-mode on fundamental electron cyclotron harmonic. $R_0=1\text{m}$, $\lambda_0=2\text{mm}$, $X=0.5$.

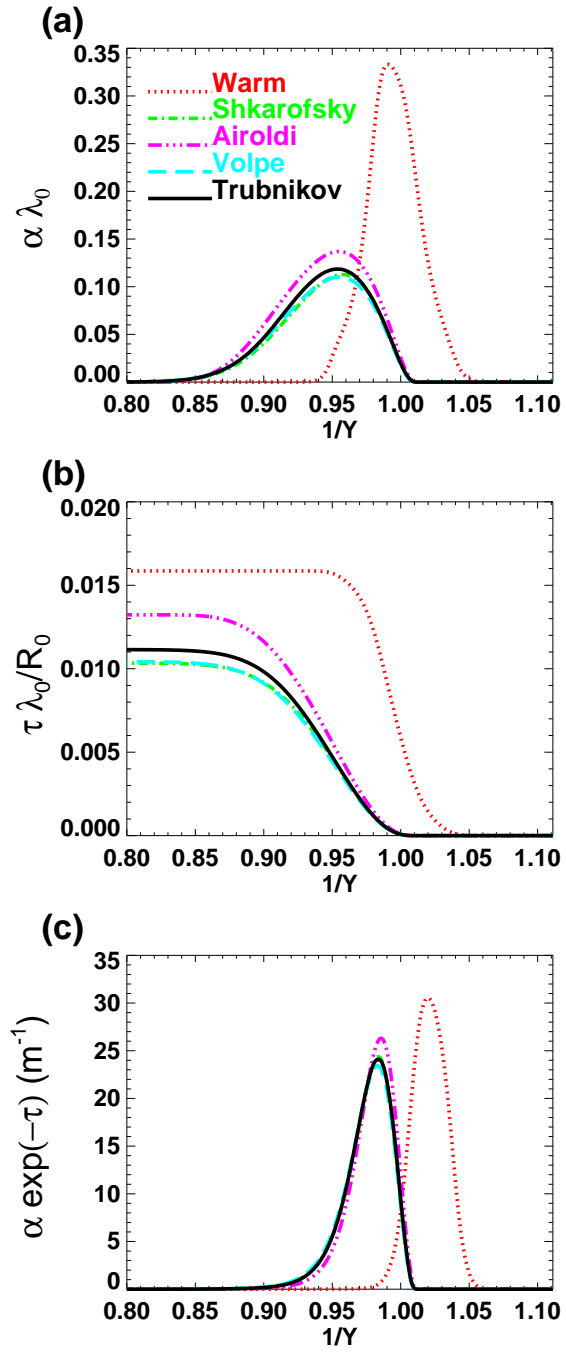


FIG. 8: (color online) Like Fig.7, except $N_{\parallel}=0.15$.

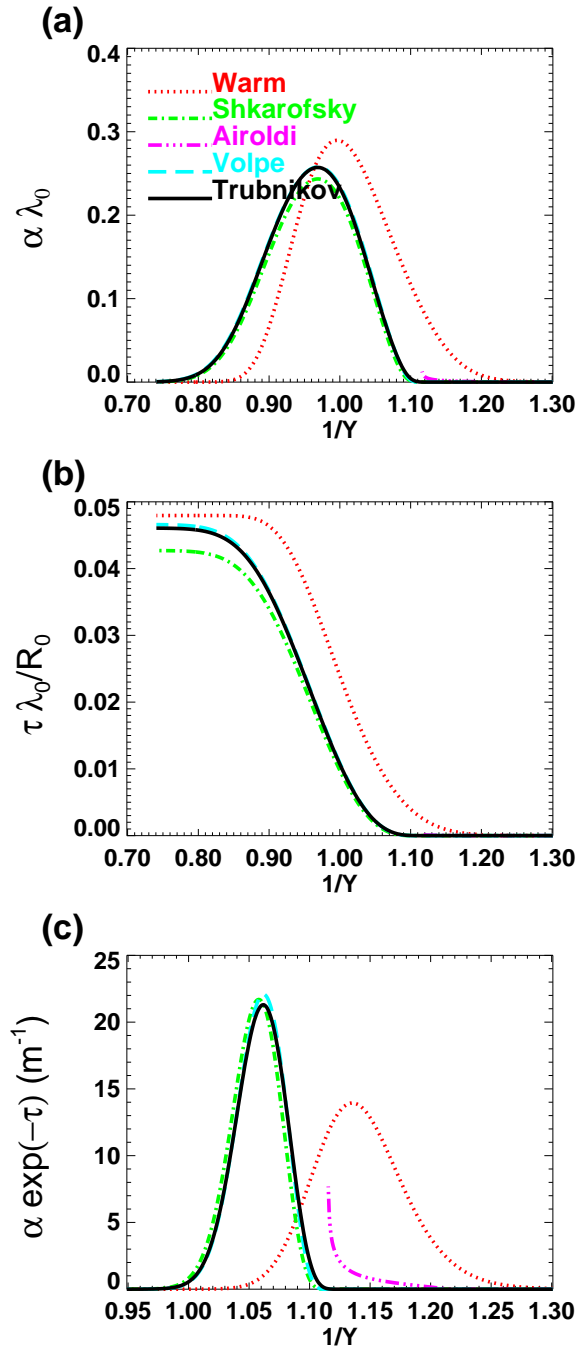


FIG. 9: (color online) Like Fig.7, but for $N_{\parallel}=0.45$, making Doppler broadening important. Note the expanded horizontal scale in Fig.c.